Rapid fabrication of a large-area close-packed quasi-periodic microlens array on BK7 glass

Feng Chen,* Zefang Deng, Qing Yang, Hao Bian, Guangqing Du, Jinhai Si, and Xun Hou

State Key Laboratory for Manufacturing System Engineering & Key Laboratory of Photonics Technology for Information of Shaanxi Province, School of Electronics & Information Engineering, Xi'an Jiaotong University, Xi'an 710049, China

**Corresponding author: chenfeng@mail.xjtu.edu.cn*

Received September 30, 2013; revised December 5, 2013; accepted December 16, 2013; posted December 20, 2013 (Doc. ID 198594); published January 28, 2014

Large-area close-packed microlens arrays (MLAs) are highly desirable for structured light and integrated optical applications. However, efficient realization of ultralarge area MLAs with a high fill factor is still technically challenging, especially on glass material. In this Letter we propose a high-efficiency MLA fabrication method using single-pulsed femtosecond laser wet etch and close-packed quasi-periodic concave MLAs consisting of three million units fabricated on silica glass within an hour. The fabricated MLAs are demonstrated to have extreme optical smoothness (~8.5 nm) by an atomic force microscope. It has also been demonstrated that the profile of the quasi-periodic concave structures could be easily tuned by changing the laser scanning speed or the pulse energy. Additionally, the optical performances of the MLA diffusers were investigated by using sharp focusing, high-resolution imaging, and flat-top illumination.

OCIS codes: (140.3330) Laser damage; (140.3390) Laser materials processing; (220.3630) Lenses; (230.1980) Diffusers; (320.2250) Femtosecond phenomena; (240.3990) Micro-optical devices.

http://dx.doi.org/10.1364/OL.39.000606

Large-scale refractive microlens arrays (MLAs) with concave surfaces have attracted enormous interest in the application of structured light and micro-optical systems and are utilized extensively in laser shaping to avoid generating local "hot spots." Recently, a variety of approaches for fabricating concave MLAs based on photolithography with expensive masks [1,2], external force [3–5], reflow technique [6], or diamond turning [7,8] have been described in the literature. However, most approaches were based on photoresist materials with a low damage threshold, which is unsuitable for high-energy laser shaping, and the distribution of the microlenses were mainly periodic, which will produce interference effects especially with the usage of highly coherent light, significantly reducing the output beam uniformity. In addition, the above-mentioned fabrication techniques are low-efficiency, technical-complex, and high cost. A high-efficiency fabrication approach that enables the surface profiles of concave microlenses controllable on silica glass is still lacking.

In this Letter, we present a facile and high-efficiency fabrication approach for fabrication of concave MLAs. The fabrication process is based on single femtosecond laser pulse irradiation and selective wet etching. Three million microlenses could be fabricated per hour, which is about 3 order of magnitudes faster than previous femtosecond laser fabrication methods [9]. To demonstrate its flexibility in fabrication of microlenses, concave MLAs of quasi-period with different profiles were fabricated on 20 mm × 20 mm silica glass blocks.

The silica glass substrates with dimensions of 20 mm × 20 mm × 2 mm were cut from a commercially available glass (BK7) sheet and were double-side polished. After ultrasonic cleaning in de-ionic water for 15 min and dried in ambient air, the glass substrate was mounted on a three-dimensional (3D) translation stage (M-505.2DG, Physik Instrumente) and irradiated in the air by a 1 kHz train of 50 fs, 800 nm laser pulses from an amplified Ti:sapphire laser. The pulse energy can be varied by the filters of different optical densities and was set to 5 μJ. The laser beam was focused by a 50×object (Nikon, NA = 0.5) before striking the surface at normal incidence. The substrate was translated in a direction perpendicular to the laser beam at a speed 20 mm/s which results in ablation craters with an average separation of 20 μm at a laser repetition ratio of 1 kHz. To create the point array, a square was fabricated along the y axis with a 20 μm transverse distance between scanning lines by having the 3D stage move the substrate. For subsequent use, the substrates were cleaned ultrasonically again in de-ionized water to remove the laser ablation ejecta.

As reported in [10] and [11], when the laser power exceeds the damage threshold of silica glass, a Coulomb explosion occurs within the silica glass at the focal spot. Consequently, a high-pressure wave generated and expanded from the focal volume [12], causing melted material from the center of the explosion to move outward and leaving behind permanent structural modifications. Previous literature indicated that the modifications in structure arose from the decrease of $O_3 \equiv Si–O–Si \equiv O_3$ bridging angles of the SiO_4 tetrahedrons [13], which could be considered in terms of the Lewis base, increasing the chemical activity in reactions with acids rather than nonmodified silica glass.

Then after a 40 min chemical treatment (at 60°C) using a 5% hydrofluoric acid solution (diluted by ionized water), close-packed concave MLAs were fabricated on the substrate surface. During this chemical etching, the craters expanded homogeneously and progressively formed circular patterns until the adjacent concave structures "squeezed" each other.

The surface morphology of the MLAs were characterized with a field emission scanning electronic microscope (FE-SEM, FEOLJSM-7000F), as shown in Figs. 1(a) and 1(b), demonstrating the extreme quality of the surface. During the laser irradiation process, the arrangement of induced craters was quasi-regular due to the

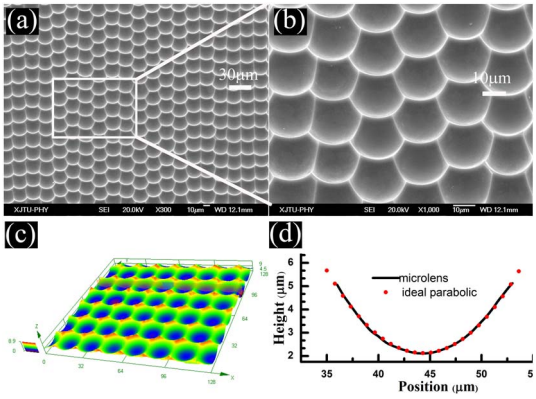

Fig. 1. 2D and 3D morphology of fabricated MLA. (a) Top-view and (b) 25° tilted-view SEM image of the quasi-periodic MLA. (c) LCSM image of the quasi-periodic MLA. (d) Actual profile of the microlens (solid line) and the ideal parabolic profile (dotted line). Note that (b) is the enlarged image of the boxed area of (a). The roughness of the concave surfaces Ra is about 8.5 nm when measured using an atomic force microscope for an area of 2 μm × 2 μm on the bottom of the sag surface.

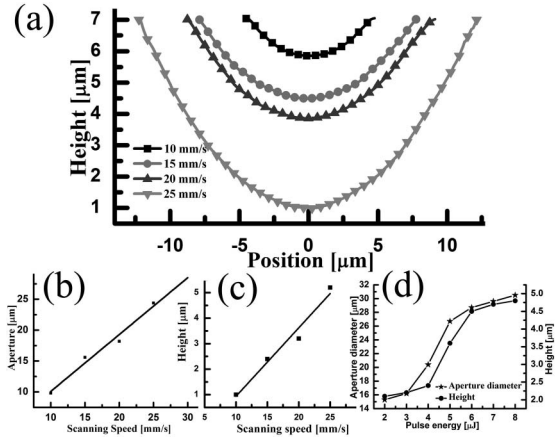

Fig. 2. (a) The profile of fabricated microlenses under different moving velocities. Graphs (b) and (c) show a change of the aperture and sag height of the microlens with the applied scanning speed, respectively. Graph (d) shows a change of the sag height (star markers) and the aperture diameter (circle markers) with the pulse energy.

vibration and the insufficient accuracy of positioning of the fast-moving 3D translation stage. Consequently, the microlens elements were also quasi-regularly arranged, as shown in Figs. 1(a) and 1(b), and the fill factors of the MLAs were closed to 100%.

Moreover, to quantify the 3D morphology of the microlenses, a laser confocal scanning microscope (LCSM, Olympus LEXT OLS4000) was employed to characterize the profile of the microlenses. Measurements in different regions demonstrated the microlens with various apertures from 18.2 to 22.4 μm, and the sag height was about 3.2 μm. The area of the fabricated MLA substrate was 2 cm × 2 cm. The microlenses were arranged in a quasi-periodic array with a fill factor close to 100%. The focal length of the microlens could be calculated according to $f = (R^2 + h^2)/2h(n-1) - h(n-1)$ [14], where R and h are the radius and height of microlens, respectively, and n is the reflective index of silica glass. Considering $n = 1.51$, we found f ranging from 27.4 to 37.1 μm.

Different profiles of the microlens can be obtained by simple adjustment of the laser scanning speed during the laser irradiation process. Cross sections of the sag surfaces for the fabricated MLAs were sampled by LSCM and are shown in Fig. 2(a) for a varying scanning speed. It is obvious that the apertures of the microlens are proportional to the scanning speed [see Fig. 2(b)] which indicates that the microlens with specifically designed size could be easily obtained by changing the scanning speed. However, the scanning speed should be larger than 5 mm/s because a lower scanning speed may not allow the craters to separate from each other.

Figure 2(c) shows the influence of the scanning speed on the sag height of the microlens. The increase of the sag height with the scanning speed was due to the fact that the laser-induced modification increased the local chemical etching rate in the longitudinal direction, and more etching time was needed for larger scanning speed. Moreover, Fig. 2(d) presents the changes of sag height and aperture diameter of the microlenses with the laser power. Here, the values were obtained from the microlenses treated by 5% HF for 30 min, which indicate that the profile of the microlenses could also be controlled by the laser power. Then, Table 1 shows the average parameters of microlenses measured from ten microlenses.

In addition, we tried using parabolic, spherical, and elliptical surfaces to fit the measured sag surface profiles. The profile of the fabricated microlenses fit very well with the ideal parabolic profile. The root mean square (RMS) deviations between the actual and ideal profile are less than 0.07 μm. It is worthy to mention that the parabolic shape of a refractive lens is particularly desirable for minimizing spherical aberration in many optical applications [14].

These smooth concave structures were characterized by a white light illumination to evaluate their ability to act as microlenses. Figure 3(b) shows a optical microscope image of the false focal point of the white light propagating through the microlenses. The average focal length f of the microlens was measured from ten microlenses to be 30 ± 5 μm, which agrees with the calculated value. In addition, we inserted a opaque mask with a transparent letter "A" between a bright light source and the MLAs, as shown in Fig. 3(a). The clear false images were observed with a CCD camera, as shown in Fig. 3(c).

Then, the illumination pattern of the fabricated periodic (rectangular and hexagonal) and quasi-periodic

Table 1. Parameters of the Microlens Measured from Ten Microlenses

Scanning Speed (mm/s)	Etching Time (min)	Diameter (μm)	Sag Height (μm)	Focus (μm)	RMS Error[a] (μm)
10	20	9.8	1.0	24.1	0.02
15	25	15.6	2.4	32.8	0.03
20	30	18.2	3.2	26.9	0.06
25	40	24.4	5.8	27.8	0.06

[a]RMS error refers to the root mean square error between the actual profile of the microlens and the ideal parabolic profile.

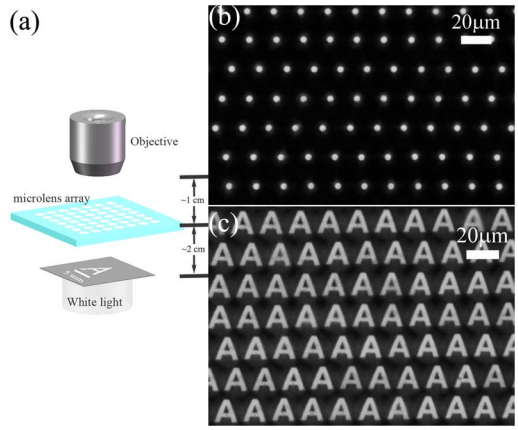

Fig. 3. (a) The optical characterization system for MLAs. (b) The false bright focal point is observed with a CCD and the focal length is measured to be about 20 μm. (c) The false images of the letter "A" with a CCD using a substrate fabricated by applying a scanning speed of 20 mm/s.

MLA diffusers were measured. The periodic MLAs were fabricated using femtosecond-laser-enhanced chemical wet etching [9], which was previously proposed by our group. A collimated He–Ne laser was used as a light source. The output beam radius from the He–Ne laser is about 0.6 mm, so we expand it to about 5 mm in order to cover the central part of the fabricated MLAs. The transmission laser beam is focused by a lens ($f = 75$ mm) and captured by a CCD camera. The CCD camera was placed 20 cm from the lens. Figures 4(a)–4(c) show the illumination pattern of rectangular, hexagonal, and quasi-periodic microlenses, respectively, with an aperture of 20 μm. The illumination patterns of periodic MLA diffusers [Figs. 4(a) and 4(b)] have demonstrated obvious interference effects.

Finally, the illumination patterns of quasi-periodic MLA diffusers with different apertures were also measured. To clarify the comparison of output intensity distributions, we normalized the intensity distributions at the central horizontal line of each pattern and plotted the curves in Fig. 5.

The incident laser intensity is a typical Gaussian distribution. After being shaped by the fabricated MLAs, the output beams are nearly flat-top, and the homogenization of the transmission pattern is increased by decreasing the diameters of the microlens elements. This increase

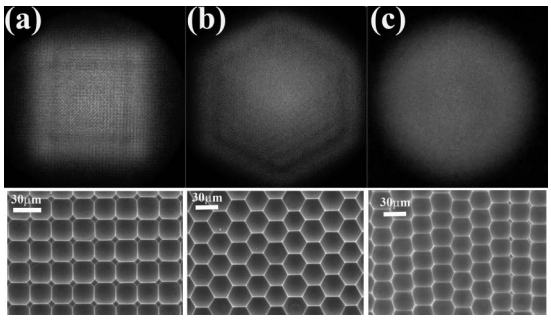

Fig. 4. Normalized intensity distribution curves at the central horizontal line of the illumination pattern of the fabricated MLAs diffuser with a He–Ne laser ($\lambda = 632.8$ nm, beam radium = 0.6 mm, and divergence angle = 1.5 mrad).

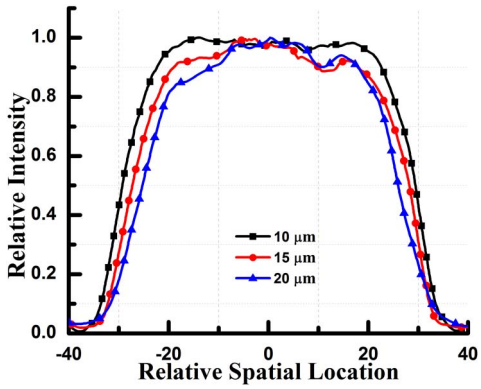

Fig. 5. Normalized intensity distribution curves at the central horizontal line of each pattern produced by fabricated quasi-periodic MLAs with different average periods of 10, 15, and 20 μm.

is reasonable according to the physical mechanism of the MLA homogenizer. The laser beam transmitted from a MLA will split into many beamlets by these multi-aperture elements followed by recombining the separated beamlets. This split-recombination process will eliminate the influence of the incident laser intensity profile, and the elimination will be improved by increasing the quantity of beamlets. Thus, quantity addition of microlens elements in a unit area will split the incident laser beam into more beamlets and will produce better uniform illumination.

In summary, a facile and high-efficiency fabrication for a high fill factor concave MLA was proposed. A quasi-periodic MLA with about several million units were easily fabricated on BK7 glass within an hour. Additionally, the diameter and sag height of the microlens can be easily controlled through the laser scanning speed. The focusing, imaging, and homogenizing properties of the MLAs were measured, and the results revealed excellent optical performance of the quasi-periodic MLAs. This large-scale quasi-periodic concave MLA would be beneficial for developing laser-based projection displays and other applications, such as LED, OLED, LCD, and laser fabrication, that require various distribution characteristics in MLA diffusers.

This work is supported by the National Science Foundation of China under Grant Nos. 51335008, 61275008, and 61176113, and the Special-Funded Program on National Key Scientific Instruments and Equipment Development of China under Grant No. 2012YQ12004706.

References

1. P. Ruffieux, T. Scharf, I. Philipoussis, H. P. Herzig, R. Voelkel, and K. J. Weible, Opt. Express **16**, 19541 (2008).
2. D. Chandra, S. Yang, and P. C. Lin, Appl. Phys. Lett. **91**, 251912 (2007).
3. X. Li, Y. Ding, J. Shao, H. Liu, and H. Tian, Opt. Lett. **36**, 4083 (2011).
4. M. B. Chan-Park, C. Yang, X. Guo, L. Q. Chen, S. F. Yoon, and J. H. Chun, Langmuir **24**, 5492 (2008).
5. X. Li, Y. Ding, J. Shao, H. Tian, and H. Liu, Adv. Mater. **24**, OP165 (2012).
6. M. He, X. Yuan, J. Bu, and W. C. Cheong, Opt. Lett. **29**, 1007 (2004).

7. A. Y. Yi and L. Li, Opt. Lett. **30**, 1707 (2005).
8. S. Scheiding, A. Y. Yi, A. Gebhardt, L. Li, S. Risse, R. Eberhardt, and A. Tünnermann, Opt. Express **19**, 23938 (2011).
9. F. Chen, H. Liu, Q. Yang, X. Wang, C. Hou, H. Bian, W. Liang, J. Si, and X. Hou, Opt. Express **18**, 20334 (2010).
10. R. R. Gattass and E. Mazur, Nat. Photonics **2**, 219 (2008).
11. A. Marcinkevičius, S. Juodkazis, M. Watanabe, M. Miwa, S. Matsuo, and H. Misawa, Opt. Lett. **26**, 277 (2001).
12. M. Sakakura, M. Terazima, Y. Shimotsuma, K. Miura, and K. Hirao, Opt. Express **15**, 5674 (2007).
13. R. A. B. Devine, R. Dupre, I. Farnan, and J. J. Caponi, Phys. Rev. B **35**, 2560 (1987).
14. D. Wu, S. Z. Wu, L. G. Niu, Q. D. Chen, R. Wang, J. F. Song, H. H. Fang, and H. B. Sun, Appl. Phys. Lett. **97**, 031109 (2010).